RESEARCH ARTICLE

INTERNATIONAL RESEARCH JOURNAL OF MULTIDISCIPLINARY TECHNOVATION

Asian Research Association

DOI: 10.54392/irjmt2616

# Study of Streptomyces extract as an effective inhibitor against microbiologically influenced corrosion by Pseudomonas aeruginosa biofilm on API 5L X52 steel

**F. Bouchakour [a, b, *], E. Driche [a], T. Unsal [c], C. Fares [d], O.S. Taskın [c], A. Aksu [c], M. Sebaihia [d]**

[a] Laboratory of Molecular Biology, Genomics and Bioinformatics (LBMGB), Faculty of Natural and Life Sciences (SNV), Hassiba Benbouali University of Chlef, Algeria

[b] Faculty of Technology, Hassiba Benbouali University of Chlef, Algeria.

[c] Institute of Marine Sciences and Management, Istanbul University, Vefa Fatih, Istanbul 34134,Turkey

[d] Laboratory of Rheology and Mechanics, Faculty of Technology, Hassiba Benbouali University of Chlef, Algeria.

* Corresponding Author Email: f.bouchakour@univ-chlef.dz

DOI: https://doi.org/10.54392/irjmt2616

Received: 07-08-2024; Revised: 09-12-2025; Accepted: 28-12-2025; Published: 13-01-2026

**Abstract:** This research investigates the effect of a Streptomyces-derived extract (SE) on microbiologically influenced corrosion (MIC) induced by Pseudomonas aeruginosa biofilms on API 5L X52 steel. Various amounts of SE were evaluated in P. aeruginosa cultures by 7-day immersion assays. SE was extracted from Actinobacteria strains found in a soil sample from the Béchar-Kenadsa region of the Sahara. Gas chromatography-mass spectrometry (GC-MS) was utilized to analyze the chemical composition of the extract. This facilitated the identification of specific components that inhibit corrosion. The anticorrosion efficacy of SE against biofilm-induced corrosion under microbiological influence (CMI) of API 5L X52 steel caused by P. aeruginosa was assessed by potentiodynamic polarization (PDP) and electrochemical impedance spectroscopy (EIS). Scanning electron microscopy (SEM) was employed to examine the surface morphology. The findings indicate that the incorporation of SE significantly inhibits the development of P. aeruginosa biofilms on the coupons. This inhibitory activity leads to a significant reduction in the rate of microbiologically induced corrosion, commonly attributed to bacterial colonization.. In silico investigations validated that the discovered compounds exhibit a strong affinity for the corrosive bacterium P. aeruginosa, elucidating their inhibitory function.

**Keywords:** Microbiologically influenced corrosion (MIC), Streptomyces extract (SE), Electrochemical impedance spectroscopy (EIS), API 5L X52, Molecular docking.

## 1. Introduction

A relatively severe issue, microbiologically induced corrosion (MIC) is a phenomenon that occurs due to the combination of microorganisms and metallic surfaces and is experienced in a wide range of industrial sectors [1-3]. According to the National Association of Corrosion Engineers (NACE), the global cost of corrosion in a single year is estimated at 2.5 trillion dollars of which 500 billion is attributed to microbiologically influenced corrosion (MIC) [4].

One of the potential corrosive agents, which have been identified, is *P. aeruginosa*. This is a gram-negative bacterium that is known to be able to form biofilms on a wide range of surfaces and stainless steel (SS) is one of them. Prominent studies, including the fundamental research.

The study by Ab and Ha (2015) [5] and the one by Cai, et al. (2021) [6] has underlined the strong connection of P. aeruginosa to biocorrosion. There are many complex processes mediated by this bacterium in the corrosion of steel: biofilm formation [7], metabolite production [8], oxygen depletion [9], passive film modification through direct enzymatic attack [10], the electrochemical properties [11], and the production of extracellular polymeric substances (EPS) [12].

These effects frequently collaborate to expedite and concentrate stainless steel corrosion in environments contaminated by *P. aeruginosa*. The corrosion process begun by *P. aeruginosa* on stainless steel surfaces entails a complicated interaction of biological and chemical factors. Recent studies show that species of Pseudomonas produce enzymes including catalase that influence oxygen reduction reactions and alter the characteristics of the passive film on the metal. The changes in the passive film as

manifested by changes in the cathodic currents illustrate the great impact enzymes have on quieting the surface of the metal [13]. *P. aeruginosa* binds to surfaces after attachment and forms an extracellular biofilm matrix. The enhanced EPS generation has a significant impact on aeration trends on surfaces of metal, and this brings about the variation in pH and redox reactions [14]. These modifications can therefore accelerate the rate of corrosion by setting up local microenvironments whose oxygen levels are not uniform and which may counteract the protective oxide covering of the metals. Moreover, the electrical conditions at the steel surface are altered due to *P. aeruginosa* and its biofilm. This results in changes in the corrosion potentials, and increased corrosion current densities, therefore, accelerating the deterioration process [15]. Furthermore, Huang et al. (2018) [16] have done a thorough study of the genetic commendations pertaining to the corrosion caused due to this bacteria. Their studies found out that the excretion of phenazine-1-carboxamide, a hydrophilic electronic shuttle that happens to be produced by the PhzH gene, stimulates the corrosion of stainless steel by means of electron transport between the bacteria and the metal. This study supplements those presented in the last years by the presence of complex mechanisms of extracellular electron transfer, molecule signaling liberation, and EPS production of *P. aeruginosa* that thereby advances the understanding of corrosion processes [17, 18].

Several methods have been used to control MIC, which have included microbiology, molecular biology, corrosion tests and electrochemical methods. Various tactics can be utilized to impede the corrosion mechanisms of *P. aeruginosa* on SS. The utilization of protective coatings [19], biofilm dispersal agents [20], biocides [21], electrochemical protection [22], chemical corrosion inhibitors [23], nanoparticles [24], and biological control by the introduction of competing, non-corrosive microorganisms [25].

Emerging technologies, including biological control approaches, demonstrate potential and have produced eco-friendly inhibitors to mitigate detrimental effects on public health and the environment. Nevertheless, the application of certain bacteriophages for biological control has been insufficiently investigated in the literature. This study seeks to produce an inhibitor derived from *P. aeruginosa* bacteriophages, motivated by unique protective strategies and informed by our prior research and other investigations. The Actinobacteria phylum was selected for its metabolic diversity, bioactive potential, and capacity to produce secondary metabolites [26] with antibacterial [27, 28], anti-biofilm [29, 30], and anticorrosive [31] capabilities. This functional variety indicates that these microbes may be essential in the development of biocorrosion inhibitors [32].

The secondary metabolites of Streptomyces display significant structural variety, encompassing polyketides, peptides, alkaloids, and terpenes [33]. Their generation and secretion are governed by intricate mechanisms reliant on certain transport networks and environmental factors. These chemicals have applications across multiple industries, including medicine and industry, and their comprehensive study facilitates the development of natural and effective solutions, rendering them potential candidates for sustainable and environmentally friendly approaches to biocorrosion management.

This study examined the effect of isolated Streptomyces extract (SE) from Actinobacteria strains sourced from a Saharan soil sample in the Bechar-Kenadsa region on the corrosion of API 5L X52 induced by *P. aeruginosa* biofilm. Electrochemical Impedance Spectroscopy (EIS) and Potentiodynamic Polarization (PDP) techniques were employed to assess the possible inhibitory effect of SE on the microbiologically influenced corrosion (MIC) of API 5L X52 alloy caused by *P. aeruginosa* biofilm. Furthermore, surface morphology characterisation via Scanning Electron Microscopy (SEM) was performed to assess the extract's effect on surface morphology.

The main objective of this work is to evaluate the potential of Streptomyces-derived bioactive metabolites as a novel and environmentally friendly strategy to inhibit *P. aeruginosa*-induced MIC on API 5L X52 steel**,** in contrast to the plant-based [34] or biosurfactant-based green inhibitors [35] commonly reported in previous studies

## 2. Materials and methods

### 2.1 Test specimens and microorganism

API 5L X52 alloy pipeline steel, commonly used in the Algerian gas pipeline network, utilized in this research. Table 1 lists the chemical makeup of the API 5L X52. The composition was ascertained by means of the SciAps X550 X-ray fluorescence spectrophotometer. For testing, the API 5L X52 steel sample preparation went through several steps: Initially, any surface contaminations were eliminated by samples undergoing a cleansing process using acetone, subsequent to washing with purified water. Next, the surfaces were meticulously refined using progressively finer grades of sandpaper-like 180, 400, 800, and 1200 grit, to achieve a flawlessly smooth finish. After polishing, the samples were thoroughly washed with distilled water to eliminate any remaining dust particles. Finally, the samples were subjected to UV radiation for 30 minutes to eradicate microbial contamination. A 1 $cm^2$ area was exposed to the bacteria and solution on the steel specimens. *P. aeruginosa* with a strain reference ATCC [27853] was used for MIC tests.

**Table 1.** Chemical composition of the API 5L X52 steel (in weight %)

| Element | C | Si | Mn | S | Cr | Ni | Mo | Cu | Al | Ti | Nb | Fe |
|---|---|---|---|---|---|---|---|---|---|---|---|---|
| Composition | 0.22 | 0.24 | 1.22 | 0.04 | 0.17 | 0.14 | 0.06 | 0.19 | 0.32 | 0.04 | 0.081 | Bal. |

The corrosive agents preparation protocol commences with preservation of stocks of *P. aeruginosa* in glycerol at -80 C, thawing and sub-culture on nutrient agar.

## 2.2 Actinobacterium strains isolation

Strains of Actinobacterium were recovered from soil samples in the Saharan region of Bechar Kenadssa utilizing chitin-vitamin agar (CHV), recommended Hayakawa & Nonomura [36]. Vitamins and antibiotics were added to this environment to adjust a pH of 7.2. This method effectively selects and isolates Actinobacteria from Saharan soils, and it can reduce the growth of contaminating bacteria and fungi. For the dilution of sample batches and the inoculation of the obtained suspensions onto Petri dishes containing CHV medium, All plates were kept at 30°C for a period ranging from 7 to 21 days to encourage the growth of Actinobacteria.

## 2.3 Antimicrobial activities of Actinomycetes bacteria extract

The antimicrobial properties of isolated SE were evaluated to identify suspected antibacterial and anti-biofilm compounds. The preliminary phase was finalized employing the cross-track plate technique as earlier documented by Driche *et al* [37], and a secondary stage was accomplished with the sound technique. The bioactive components of the selected Streptomyces strain in the first stage were extracted to assess their effectiveness against the *P. aeruginosa* bacteria ATCC [27853]. To generate extracellular metabolites, 50 mL of a modified medium (mineral- enriched Yeast Glucose Broth) containing 7 g/L of glucose, 1 g/L of yeast extract, 40.1 g/L of $MgSO_4$, 40.3 g/L of $KH_2PO_4$, 5 g/L of NaCl, and 30.5 g/L of $CaCO_3$, was used., to cultivate Streptomyces isolate for 7 days at 30 °C. Then, the fermentation medium was centrifugated at 7656 ×g to create a sergeant devoid of cells for 15 to 20 minutes. This surfactant has been mixed with the same amount of ethyl acetate solvent, frequently used to extract Actinobacterial metabolites. Following the organic and aqueous phase separation, the molecules were extracted from the organic layer and dried in preparation for additional study. The ethyl acetate was completely removed using a rotary evaporator before the extract was applied to bacterial cultures and corrosion tests. Experiments have been conducted to examine the impact of varying extract concentrations on bacterial proliferation and biofilm development.

## 2.4 Identifying the isolated bacteria

A 5 mL volume of pure culture during the exponential growth phase was centrifuged at 15,000 x g to pellet the cells. Genomic DNA was extracted using the DNeasy PowerSoil Kit (Qiagen) according to the manufacturer's [38]. The universal bacterial 16S rRNA primers, PU1 (5-182 TGA TCC TGG CTC AG-3-) and PU2 (5-182 GGT TAC CTT GTT ACG ACT T-3-) served as PCR primers. The PCR reaction (25 µ L final volume) contained the BIOTAQ MasterMix (Bioline) [39], primers PU1 and PU2, and that of the DNA template. PCRs were amplified using a T100 thermocycler (Bio-Rad) at the following conditions: an initial denaturation of 94 o C in 3 min; 35 cycles of 94 o C for 30 s (denaturation), 55 o C for 30 s (annealing), 72 o C 1 min (extension); a final extension at 72°C 5 min. The PCR products were also cleaned up by Wizard SV Gel and PCR Clean-Up system (Promega). Sanger sequencing was done at AGRF The generated sequences were searched in GenBank database by employing the BLASTn to identify the species [40].

## 2.5 Immersion tests

Immersion tests were conducted in *P. aeruginosa* culture medium with and without SE. Sterile vials (200 mL) were used for immersion tests. The vials were filled with 100 mL standard LB (Luria-Bertani) medium inoculated with *P. aeruginosa.* Before inoculation, the *P. aeruginosa* culture was diluted in Minimal Salt Medium (MSC medium) to reach an optical density ($OD_{600}$) of 1 mL seed culture containing variable concentrations of SE (100, 150, 200, and 250 µg/mL). Subsequently, five duplicate coupons were inserted into the vials. The vials were sealed and kept at 30 °C for 7 days. All experiments were conducted under sterile circumstances. The optical density (OD) of cell development was assessed via ultraviolet-visible spectrophotometry (U.V-Vis) (Shimatzu), and the pH values of the culture media were evaluated using a pH meter (METTLER TOLEDO). To enumerate sessile cells, the coupons wfigurere rinsed in phosphate-buffered saline (PBS) solution (pH 7.4) to eliminate planktonic cells, followed by swabbing the whole surface of the coupons. The biofilm biomass was vortexed in PBS solution and subsequently serially diluted to 10^7 to quantify sessile cells. Nutrient agar plates were

incubated at 37°C. All tests were conducted in duplicate. Following the incubation, the quantity of viable cells (CFU/mL) was determined.

### 2.6 Surface analysis

All the coupons were analyzed using a Scanning Electron Microscopy (SEM) (Quanta 250). All the samples were prepared as follows: the coupons with biofilm were fixed in a 2.5% glutaraldehyde solution at 4 °C for 1 h. For the cell's dehydration and stabilization on the surface, the coupons were subjected to a graded ethanol series (35, 50, 75, 90, 100%) three times for 15 min. per step.

### 2.7 Electrochemical measurements

The MIC behaviour of API 5L X52 samples in *P. aeruginosa* culture medium and without SE was also examined by employing the electrochemical techniques. Electrochemical studies were carried out using VersaSTAT 3 potentiostat with Versastudio software, a three-electrode cell. The working electrode (WE) was API 5L X52 steel, and counter electrode (CE) was a platinum sheet (10 x10 x 0.1 mm) and saturated calomel electrode (SCE) was used as a reference electrode. Once the OCP system has become stable (approximately 1 hour), EIS measurements were conducted over a frequency range of 10 -2 Hz-1 to 10 5 Hz by applying a sinusoidal signal of 10 mV. The impedance data were analysed by plotting Nyquist with ZsimpWin software. PDP was measured at a scan rate of 1 mV/s at a range of a potential (pm) of +/- 0.8 mV relative to the OCP. PDP curves were used to determine the Icorr values under different mediums (control, *P. aeruginosa* culture with and without SE).

### 2.8 Analysis of the active compounds in the culture extract of Actinomycetes bacteria

The ethyl acetate extract from Actinobacteria cultures was prepared and concentrated using vacuum evaporation for the active compounds analysis. The sample was extracted by dichloromethane (DCM) at 4ºC. The extracted content was concentrated by vapourization with a rotary, and then it was completed to 5 mL with hexane. Analysis was performed using GC/MS using an HP 6890 GC system, fitted with a capillary column (HP PONA, methyl siloxane glass capillary column). The gas chromatography initial oven temperature was established at 40°C, ramping at 10°C/min to 290°C (with a 10-minute hold), followed by a further increase at 10°C/min to 320°C (also with a 10-minute hold), culminating in a total runtime of 48 minutes.

The flow rate of the carrier gas (helium) was established at 1.2 mL/min. The temperature of the MS detector is 320°C. The temperature of the injection port is 240°C. The mass spectra were compared to a standard mass spectrum library for compound identification. Each component was identified according to its retention time and corresponding mass spectrum. The results determine the chemical composition of the active metabolites produced by potentially beneficial Actinobacteria, thereby furnishing critical information regarding the bioactive compounds present in the ethyl acetate extract.

### 2.9 Molecular docking

Molecular docking is a method that forecasts the compatibility of ligands with the binding site of target proteins. In order to achieve optimal docking, it is necessary to increase the number of proteins and establish a matrix. The target protein, *P. aeruginosa* (PDB ID: 6V7X), was obtained from the Protein Data Bank. The three-dimensional structure of the "Casadabanvirus DMS3, *Pseudomonas aeruginosa* UCBPP PA14" protein was enhanced by the Protein Preparation Wizard program from Maestro version 11.1 after it was crystallized using X-ray diffraction.This refinement process involved eliminating water molecules, enhancing hydrogen bonds, and minimizing heavy atoms with an RMSD of 0.30 Å, employing the OPLS force field. A grid was generated to identify the region of the receptor protein likely to host binding interactions. The grid's central coordinates were set at X = 18.91, Y = -3.54, and Z = -4.15, with a 20 Å extension in all directions, thus enabling the capture of potential ligand interactions at the binding site. The standard ligand N3-ODDHL was incorporated for comparative analysis. Prior to molecular docking, the geometry of each ligand was tuned. The molecular docking procedure was executed with AutoDock Vina, a software acclaimed for its superior speed and precision, attributed to its effective optimization, multithreading capabilities, and a novel scoring system [41]. The docking procedure had multiple phases, including High-Throughput Virtual Screening (HTVS), Standard Precision (SP), and Extra Precision (XP).

## 3. Results and Discussion

This study evaluated the efficacy of SE extract in inhibiting *P. aeruginosa* biofilm development and its anti-corrosive properties on API 5L X52. The efficacy of the most promising isolate was further examined through a multimodal approach that included chemical analysis, molecular identification techniques, microbiological procedures, and surface examinations. In silico modeling and electrochemical assays were employed to assess the inhibitory capability of the most effective isolate against *P. aeruginosa*.

### 3.1 Isolation of Actinobacteria

Forty morphologically distinct isolates were successfully isolated using a Nutrient Agar medium from the soil of Bechar Kenadssa for 10 to 16 days to isolate Actinobacteria. Isolates were expressed as differences in colony morphology and their colors, such as gray, white, and pink. The isolates differed in their pattern of spore chain morphology and range of pigment production. These isolates, designated ABK 1 to ABK 40, were further maintained on ISP 2 agar medium for additional investigation.

### 3.2 Antimicrobial activity screening

The initial screening was performed with a cross-test against the *P. aeruginosa* strain. The most promising isolate, ABK34, was selected for further investigation. Further, these extracellular bioactive compounds from the isolate were screened for anti-biofilm and antibacterial activity following fermentation and extraction.

### 3.3 Molecular identification of Actinomycetes

BlastN determined that the 16S rRNA sequencing analysis of ABK 34 exhibited a 99% similarity. This indicated that the isolates may be members of the Streptomyces genus. The sequence analysis indicated that GenBank contained 80% of the GC content, as indicated by the accession number PP064007. The isolate was identified as *Streptomyces qinglanensis* strain ABK34 in the present study. This strain was recently identified in a sediment sample collected from the coast of Dokdo Island and is a potential source of antibacterial compounds. According to Cao Van Anh *et al*. [42], the *Streptomyces qinglanensis* strain generated bioactive compounds that impeded the growth of a variety of Gram-positive bacteria and moderately suppressed the growth of specific Gram-negative bacteria.

### 3.4 Immersion Tests

We conducted immersion tests over a duration of 7 days to evaluate the impact of varying concentrations of SE (100, 150, 200, and 250 µg/mL) on the proliferation of *P. aeruginosa* on API 5L X52. Figure 1 illustrates the outcomes for OD600. The OD600 values increased throughout the initial days, with SE concentrations ranging from 100 to 250 µg/mL. The extract's efficacy in disrupting *P. aeruginosa* biofilms is what led to the increase. This resulted in the discharge of many cells into the culturing medium. Following the first increase, OD600 values stabilized, presumably due to antibacterial activity that inhibited growth in suspension. The results for SE concentrations between 150 µg/mL and 250 µg/mL were strikingly similar, approximating a threshold of effectiveness. Consequently, any increase in the concentration above this threshold did not augment the antibacterial effect. In this case, the number of sessile cells significantly diminished as the extract concentration increased. These results demonstrated that the extract has a dual action: biofilm disruption (leading to an initial increase in planktonic cells) and overall bacterial growth reduction (due to its antibacterial effect). The pH readings were recorded over a duration of 7 days (Figure 2). Figure 2 demonstrates that there was no considerable variation in pH levels across the various extract concentrations over a period of 7 days. The results indicated that the addition of SE did not alter the pH of the culture medium. This may also indicate that no acidic metabolites were produced throughout the treatment. The pH stability suggests that any influence on bacterial growth or biofilm

Formation cannot be attributable to increased medium acidity.

### 3.5 Electrochemical Tests

We discussed the electrochemical properties of API 5L X52L surface following the adhesion of *P. aeruginosa* growth, employing EIS and PDP, with and without SE. The Nyquist plots of electrochemical impedance spectroscopy of all the coupons are given in Figure 3. The half semicircles reflect the varying levels of corrosion resistance shown by the coupons. As shown by the sterile media, referred as the control coupon, the greatest semicircular diameter exhibits the most corrosion resistance. The corrosion resistance presented the smallest diameter of semicircle in the presence of *P. aeruginosa* implying the eroded passive properties of API 5L X52 over the 168 hours. After addition of SE, the control coupon retained the largest semicircle diameter, which implies that the control coupon retained the passive surface properties of API 5L X52 steel. According to DP analysis (Figure 4) and data (Table 2), the corrosion current densities were significantly higher when *P. aeruginosa* culture was present (703 0A/cm$^2$) than when it was absent (0.050 A/cm$^2$) or with SE co-present (0.060 A/cm$^2$). This shows that the combination of SE largely reduces MIC of *P. aeruginosa* biofilm. The immersion test data is supported by the electrochemical data, which can be used to determine that the extract acts not only as an antibacterial agent, but also as corrosion inhibitor. According to the findings, the SE could be used to interfere with bacterial growth and corrosion activity in industries where corrosion of *P. aeruginosa* is a problem. Figure 4 reveals that SE acts as a mixed-type inhibitor because the corrosion potential ($E_{corr}$) differs when using Streptomyces extract as an inhibitor and when *P. aeruginosa* strain is not applied as an inhibitor. The magnitude in the range between anodic and cathodic reaction showed a 0.17 mV change in the positive order in the presence of the extract hence being influential on both reactions [43].

Kramers-Kronig (KK) transformations were applied to validate the EIS experimental data.

The software provided goodness-of-fit values, which were determined using the chi-squared statistic [44]. This method calculates the standard deviation between the original data and the calculated spectrum. A chi-squared value of $10^{-5}$ indicates a reasonable to good fit when data without variances are used [45].

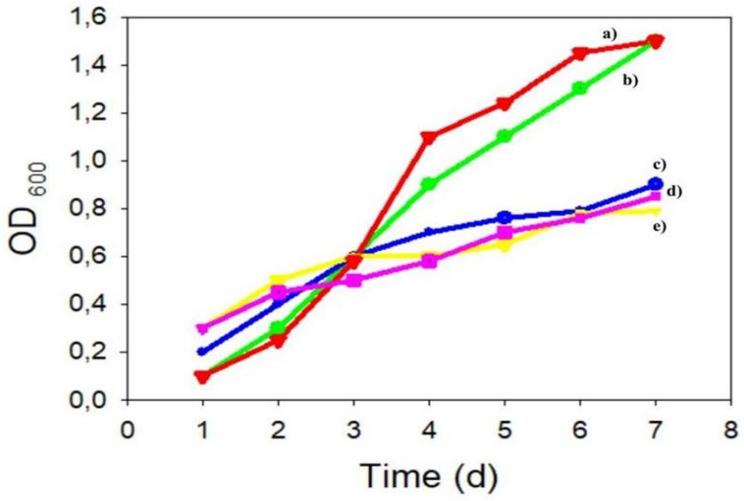


**Figure 1.** Growth curves of P. aeruginosa cells in culture media with SE of 0 µg/mL (a), 100 µg/mL (b),150 µg/mL(c), 200 µg/mL (d)( and 250 µg/mL(e).

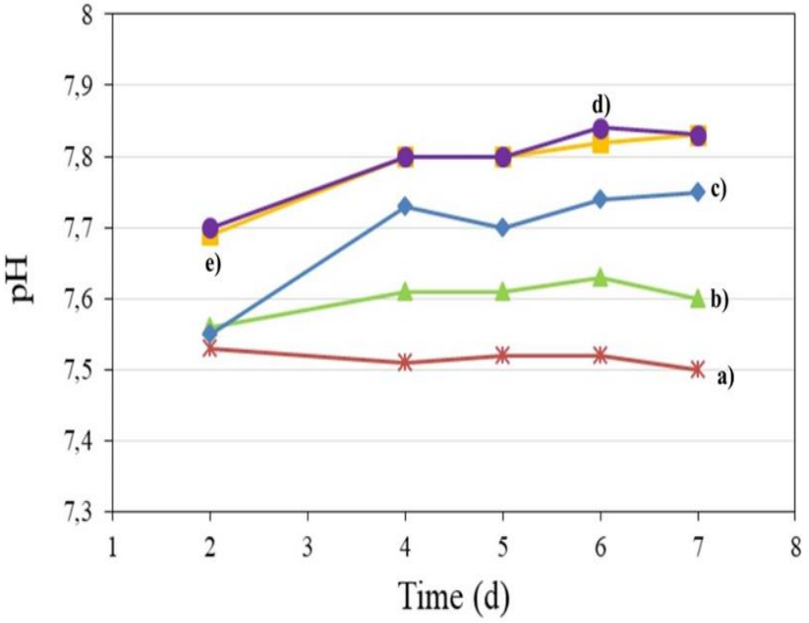


**Figure 2.** Evolution of the pH values of the *P. aeruginosa* culture media with SE concentrations of a) 0 µg/mL (red line), b) 100 µg/mL (green line), c) 150 µg/mL (blue line),d) 200µg/mL (yellow line) and e) 250 µg/mL (purple line).

**Table 2.** Fitted electrochemical parameters potentiodynamic polarization curves of API 5LX52 in Figure 4.

| Parameter | Control coupon | No treatment | with SE (150 µg/mL) |
|---|---|---|---|
| $i_{corr}$ (µA/cm$^2$) | 0.05 | 703 | 0.06 |
| $E_{corr}$ (V) vs. SCE | −0.48 | −0.77 | −0.94 |
| $\beta_a$ (V/dec) | 0.87 | 0.53 | 0.81 |
| $\beta_c$ (V/dec) | 0.313 | 0.448 | 0.43 |

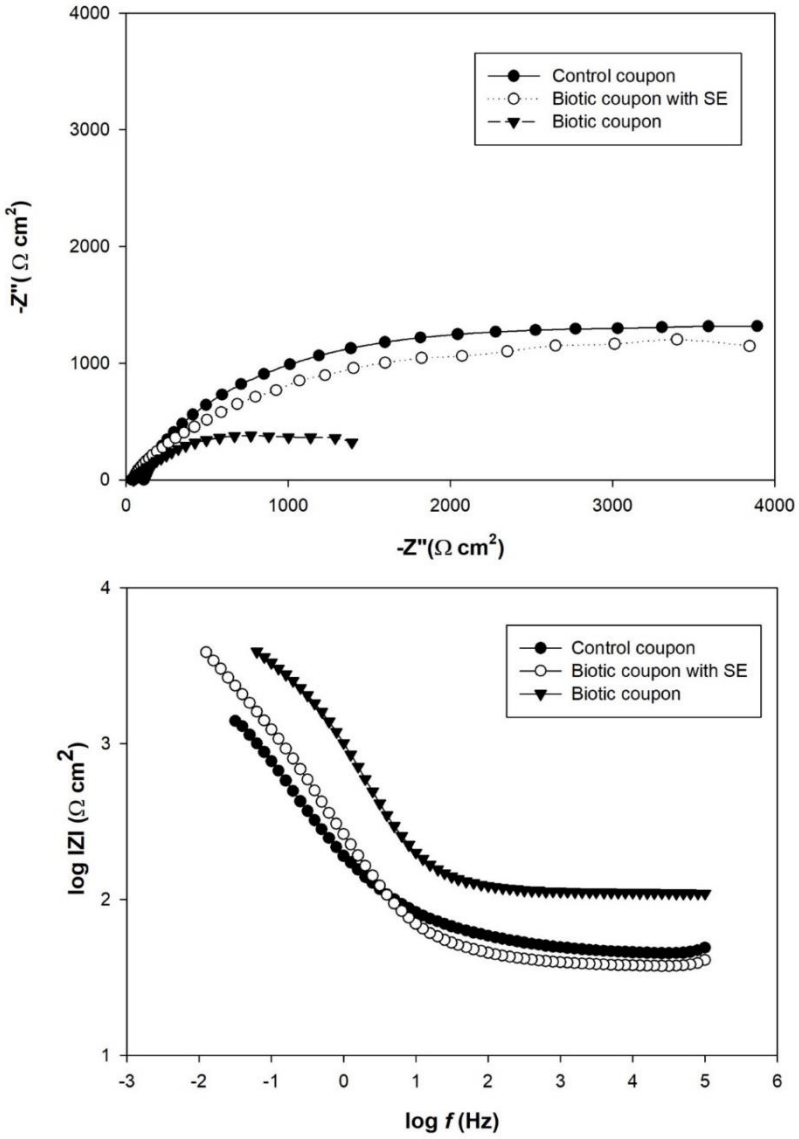


**Figure 3.** Nyquist plots and Bode plots of the control, biotic coupon and biotic coupon with SE after 7 days of immersion.

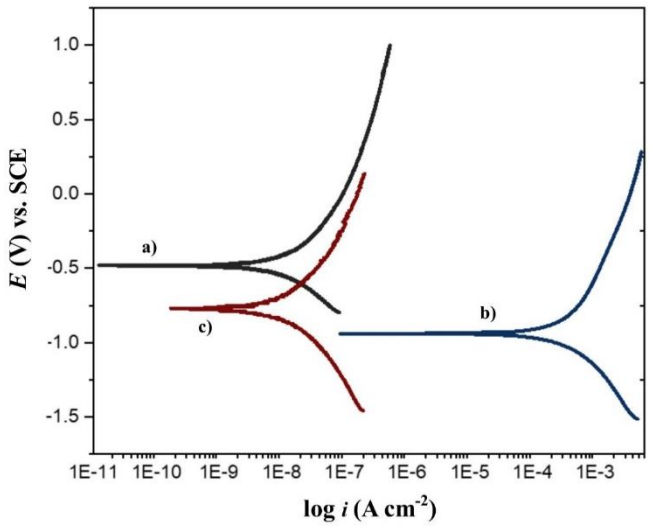


**Figure 4.** Potentiodynamic polarization curves in a) control medium, b) *P. aeruginosa* culture medium and c) *P. aeruginosa* culture medium with SE (150 µg/mL) after 7 days incubation

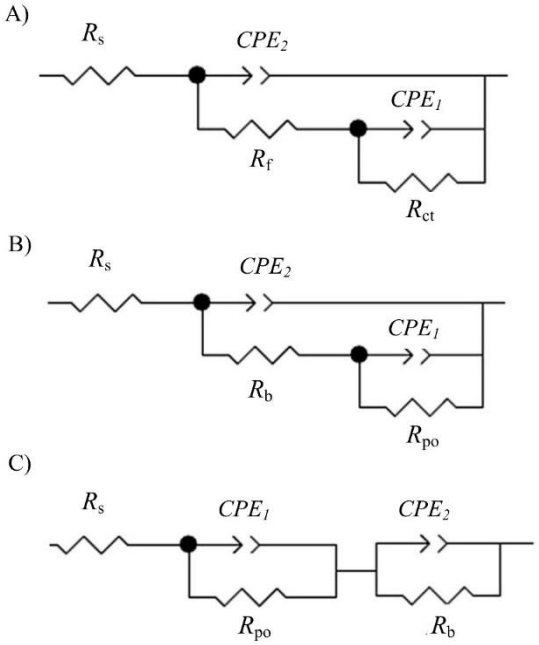


**Figure 5.** Equivalent circuits used for simulating the impedance spectra for control coupon (A) no treatment coupon (*P. aeuroginosa* culture medium) (B), with 150 µg/mL SE treatment coupon (C).

**Table 3.** Electrochemical parameters obtained from fitting EIS spectra in Figure 3.

| Coupons (7 days) | $R_s$ (Ω cm$^2$) | $Y_2$ ($\Omega^{-1}$ cm$^{-2}$ s$^n$) | $n_2$ | $R_b$ (Ω cm$^2$) | $Y_1$ ($\Omega^{-1}$ cm$^{-2}$ s$^n$) | $n_1$ | $R_{po}$ (Ω cm$^2$) |
|---|---|---|---|---|---|---|---|
| Control | 16 | 0.0216 | 0.42 | 3486 ($R_f$) | 0.0189 | 0.46 | 418($R_{ct}$) |
| No treatment | 33 | 0.0529 | 0.76 | 1328 | 0.0306 | 0.78 | 104 |
| with SE (150 µg/mL) | 25 | 0.0496 | 0.38 | 3343 | 0.0093 | 0.51 | 580 |

**Table 4.** Docking results of Lig1, Lig2, Lig3 and standard ligand (N3-ODDHL) with the target protein PDB ID: (6V7X).

| **Ligand name** | **Docking Score (kcal/mol)** | **Glide energy (kcal/mol)** | ***Hydrogen bonding*** | **Glide ligand efficiency (kcal/mol/atom)** | ***Van der Waals forces* (kcal/mol)** | **Amino acids** |
|---|---|---|---|---|---|---|
| **Lig1** | -2.90 | -22.15 | -1.04 | -0.41 | -13.91 | TRP60 |
| **Lig2** | -4.51 | -27.11 | -0.70 | -0.41 | -23.98 | TRP60, TYR93 |
| **Lig3** | -5.89 | -27.52 | -1.15 | -0.39 | -24.64 | TRP60, SER129 |
| **N3-ODDHL** | -9.26 | -53.98 | -2.30 | -0.44 | -43.65 | TYR56*, TYR93, SER129*, ASP73 |

***(Two hydrogen bonding of amino acid interactions with the same atom of the ligand)**

**N3-ODDHL:** N-3-Oxo-Dodecanoyl-L-Homoserine Lactone

**Lig1:** Propanoic acid,3-(methylthio)

**Lig2:** Pyrrolo[1,2-a] pyrazine-1,4-dione-

**Lig3:** hexahydro-3-(2-methylpropyl)-1,4-diaza-2,5-dioxo-3-isobutyl bicyclo [4.3.0] nonane

In this study, the chi-squared variance of the measurements ranged from $10^{-3}$ to $10^{-4}$. For all data the goodness-of-fit values were approximately $10^{-4}$, indicating that these values fall within the acceptable range. The EIS data was then analyzed in terms of model electrical circuits (Figure 5). A non-ideal behaviour can be modelled through a constant phase element (CPE), when the capacitors are not ideal. The CPE in standard impedance expression is written as:

$$Z_{CPE}=1/Y_0(j\omega)^n \quad (1)$$

The parameters Y 0 and n refer to the CPE; omega refers to the angular frequency. At n = 1 the CPE acts as a capacitor. When n = 0 it acts like an ideal resistor. The electrochemical values, obtained based on the EIS spectra are illustrated in Table 3. Analogous circuit of the control coupon is represented in Figure 5A. The circuit includes three elements: (1) the solution resistance ($R_s$), (2) the parallel combination of the charge transfer resistance ($R_{ct}$) and $CPE_1$, related to the capacitance of API 5L X52 steel surface double layer, and (3) the parallel combination of the film resistance ($R_f$) and $CPE_2$, which relate to the API 5L X52 steel surface conditioning film. Figure 5B represents a coupon that has not been treated, just water extract of *P. aeruginosa* culture media. A circuit with three elements can be considered: (1) $R_s$, (2) the parallel combination of $R_{po}$ and $CPE_1$, representing a heterogeneous layer comprising corrosion products, and (3) the parallel combination of that of $R_b$ and $CPE_2$, the biofilm itself. This shows Figure 5C of the treatment coupon loaded with 150 ug/ml SE. The components in the circuit are as follows: solution resistance ($R_s$), pore resistance ($R_{po}$) that consists of charge transfer resistance ($R_{ct}$) and constant phase element 1($CPE_1$) that represents the electrical double layer and constant phase element 2 ($CPE_2$) that represents biofilm resistance ($R_b$) on API 5L X52 steel. Table 5 ranks SE among the top-performing biogenic inhibitors (2020-2025), demonstrating the innovation of our strategy.

### 3.6 GC-MS Analysis Results of the Bacterial Fermentation Extract

The GC-MS analysis chromatogram (Figure 6) storied the approximately sixty-two (62) different chemical compounds characteristic feature of crude extract from *Streptomyces qinglanensis* second metabolite extracted using ethyl acetate medium (Figure 6).

**Table 5.** Comparison of biogenic inhibitors: biofilm and corrosion inhibition performance (2020-2025)

| Biogenic Inhibitor | Bacterial Source | Biofilm Inhibition (%) | Corrosion Inhibition (%) (Icorr) | Tested Material | Reference Date |
|---|---|---|---|---|---|
| SE(*S. qinglanensis*) | *Streptomyces qinglanensis*ABK34 | 85-90% (OD600 + sessile cells) | 99% (703 → 0.060 µA/cm²) | API 5L X52 | 2025 this work |
| ε-Polylysine (E-PL) | Synthetic | >90% | 85% | Carbon steel Q235 | [46] 202 |
| Cu15Zn (aged brass) | Copper alloy | 70-90% (CFU) | 75-85% | Copper | [47] 2024 |
| Plasma-Activated Water | Plasma $H_2O$ | 65-80% | 70% | Mild steel | [48] 2022 |

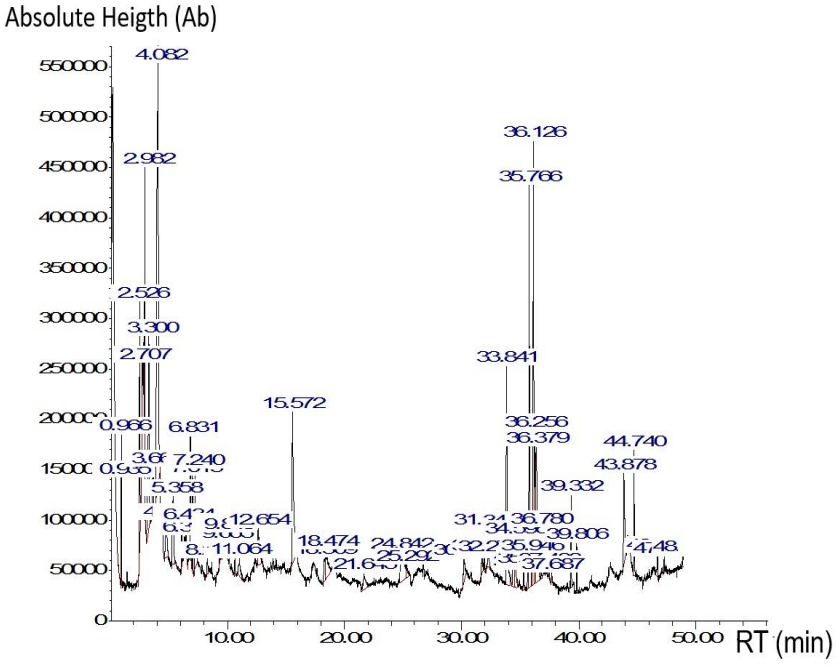


**Figure 6.** Detection of complete chemical composition of purified Actinomycete extract by GC-MS

This indicates a complex mixture of compounds in the extract, which could contribute to various biological activities. These 62 chemical compounds must be identified for biological control methods between the molecules that develop antimicrobial, antifungal, and antibiofilm and corrosion-inhibiting properties [49, 50].

Table 6 summarizes the main GC-MS identified compounds and their reported activities**,** Therefore, according to the peak intensities, peak area percentage, retention time, and potential biological activities, the selected compounds were:

**Table 6.** Main GC-MS identified compounds from SE extract and their reported activities

| N ° | Name | molecular formula | Mol Weight (g/mol) | RT (min) | Area (Ab*s) | Chemical class | Activity/Function (References) |
|---|---|---|---|---|---|---|---|
| 01 | 1,3-Dioxan-5-ol (5-Hydroxy-1,3-dioxane) | $C_4H_8O_3$ | 104.10 | 2.526 | 7047542 | Oxygen-containing heterocyclic compound (cyclic ether) | Organic synthesis solvent [51] |
| 02 | Nitromethane | $CH_3NO_2$ | 61.04 | 2.709 | 1064300 | Nitroalkane | polar aprotic solvent, chemical intermediate, ion solvation agent. [52] |
| 03 | Hydrazine, 1,2-dimethyl- (s-Dimethylhydrazine, Hydrazomethane, SDMH) | $C_2H_8N_2$ | 60.10 | 2.985 | 9353341 | Dialkylhydrazine derivative | DNA alkylating agent, research carcinogen [53] |
| 04 | Acetol (1-hydroxy-2-propanone) | $C_3H_6O_2$ | 74.08 | 3.302 | 12207858 | Hydroxy ketone | Chemical intermediate; biomass-derived precursor [54] |
| 05 | 3-(Methylthio)propionic acid | $C_4H_8O_2S$ | 120.17 | 4.083 | 41760409 | Organosulfur carboxylic acid | Antifungal activity And antibacterial activity [55] |
| 06 | Anhydro-sugar | $C_6H_{10}O_5$ | 162.14 | 15.570 | 11420255 | Sugar derivative | Reactive carbohydrate intermediates [56] |
| 07 | 3,5-Dimethyl-2-methoxy-4-pyrimidinone | $C_7H_{10}N_2O_2$ | 154.17 | 33.843 | 13747803 | Substituted pyrimidinone | antimicrobial, antiviral, anticancer, antidiabetic, anti-inflammatory, anticonvulsive, and antihistaminic effects [57] |
| 08 | 1-Naphthoic acid | $C_{11}H_8O_2$ | 172.18 | 35.641 | 778616 | Aromatic carboxylic acid | Used in dye and pharmaceutical synthesis; related naphthoic acids [58, 59] |
| 09 | Hexahydro-3-(2-methylpropyl)-pyrrolo[1,2-a]pyrazine-1,4-dione | $C_{11}H_{18}N_2O_2$ | 210.27 | 35.764 | 17543183 | Diketopiperazine (DKP) | antimicrobial, anti-biofilm, antioxidant, [60, 61] |
| 10 | 1,4-Diaza-2,5-dioxo-3-isobutyl bicyclo[4.3.0]nonane | $C_{13}H_{20}N_2O_2$ | 236.31 | 36.126 | 24065329 | Bicyclic diketopiperazine | anti-biofilm, antimicrobial, [62, 63] |

- 3-(methylthio) propanoic acid: The retention time RT: 4.083 min.
- Pyrrolo[1,2-a] pyrazine-1,4-dione hexahydro-3-(2-methylpropyl): The retention time RT: 35.764 min exhibits significant potential due to its chemical structure associated with biological activities, including antibacterial and antifungal activities [64].
- 14-diaza-2, 5-dioxo-3-isobutyl bicyclo [4.3.0] nonane: The retention time of 36.126 min, this molecule has chemical characteristics that are potentially required for inhibiting the growth of *P. aeruginosa*, a crucial microbial pathogen [65].

### 3.7 Surface morphology

The surface morphology of samples in the control medium, culture medium, and culture medium with SE was illustrated in Figure 7. Under sterile conditions, after 7 days of immersion, the surface morphology of the samples remained unaffected, with no biofilm formation.

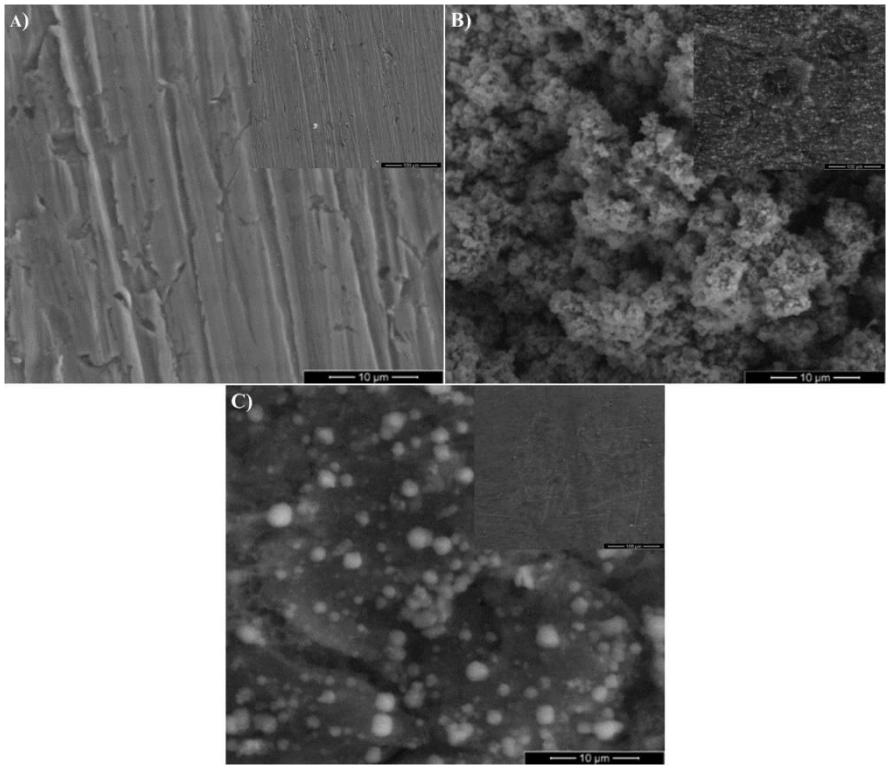


**Figure 7.** SEM images of coupon surfaces after 7 days of immersion in A) control medium, B) P. aeruginosa culture medium and C) inoculated culture medium with SE (150 µg/mL).

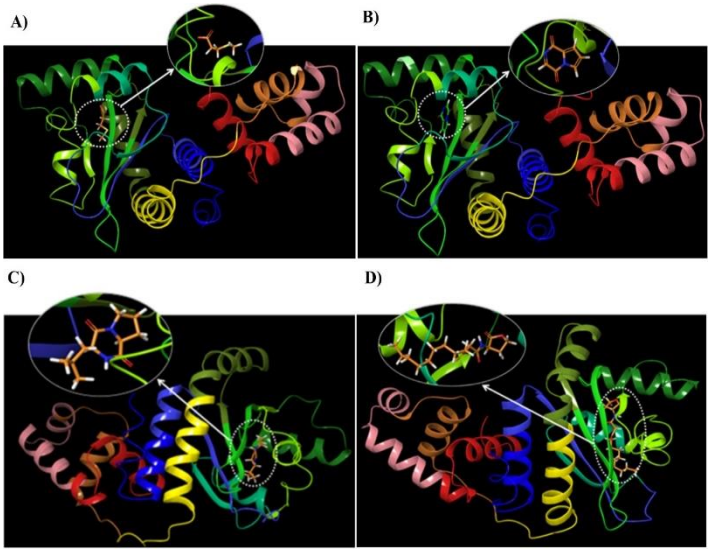


**Figure 8.** Visualization of the best docking poses of A) Lig1, B) Lig2, C) Lig3 and D) N3- ODDHL with the target protein PDB ID: (6V7X).

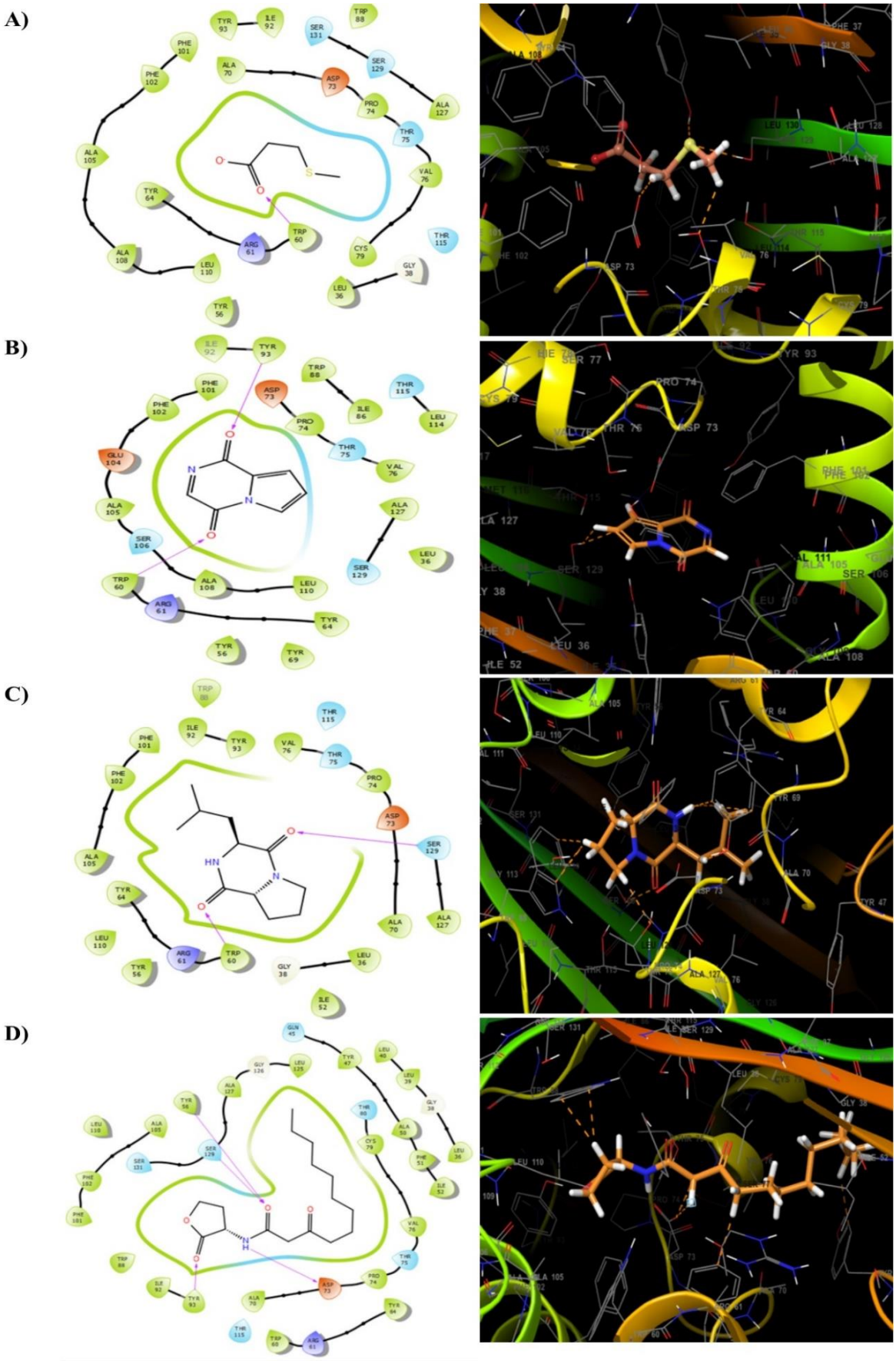


**Figure 9.** 2D and 3D interaction diagrams of the a) Lig1, b) Lig2, c) Lig3 and d) N3-ODDHL with the target protein PDB ID: (6V7X).

However, the surface morphologies were highly different in the case of the *P. aeruginosa* culture medium, in which the biofilms further appeared. Biofilms were prominently visible on localized areas of the coupon surfaces, showing localized corrosion. In contrast, No biofilm development was observed on the sample surfaces submerged in the *P. aeruginosa* culture medium that included SE. SEM images presented direct visual proof of the efficiency of this extract in preventing biofilm formation on coupon surfaces.

### 3.8 In silico analysis

The study findings demonstrated the inhibitory potential of SE on bio-corrosion induced by *P. aeruginosa* biofilm. Therefore, in silico modeling targets the provision of more profound insight into inhibition at a molecular level and the discovery of more effective lead compounds through structural optimization. The following ligands of SE are depicted by a molecular docking study represented by the docking scores against the target protein *P. aeruginosa* with the protein target (PDB ID: 6V7X), which is listed in Table 4 and Figure 8 and Figure 9. The standard ligand, N3-ODDHL, has the highest docking score of -9.26 with strong hydrogen bonding with critical residues such as TYR56, TYR93, SER129, and ASP73, showing significant Van der Waals interactions of -43.65 and sliding energy of -53.98, stating that the stability will be strong. Lig1: propanoic acid, 3-(methylthio) - had a docking score of -2.90, Lig2: pyrrolo [1,2-a]) with a docking score of of -4.51, Lig3: hexahydro-3-(2- methylpropyl)-1,4-diaza-2,5-dioxo-3-isobutyl bicyclo[4.3.0] nonane has a docking score of - 5.89.

The interaction of ligands from SE with *P. aeruginosa* protein targets presents interesting insight into the docking scores and the interaction of various ligands. Even though their interaction scores were lower, Lig3, Lig2, and Lig1 showed considerable interaction with the target protein and may act as an inhibitor. Results revealed the components' very promising inhibitory action, which probably need slight structural changes for maximum activity. These observations were in correlation with previously performed studies [41, 66] considering hydrogen and van der Waals interactions decisive for the stability of the ligand-protein complex.

The docking results, ranging from −2.90 to −5.89 kcal/mol, indicate only moderate binding compared to the standard ligand, and should therefore be interpreted with caution. Moreover, potential synergistic interactions among multiple SE metabolites may contribute to the overall effect, highlighting the importance of considering combined metabolite activity rather than focusing solely on individual ligands [67].

## 4. Conclusion

We employed immersion tests, electrochemical measurements, and surface analysis to determine the impact of secondary metabolites from the bacteria *S. qinglanensis* on the MIC of API 5L X52 induced by *P. aeruginosa* biofilm. The identification of essential chemicals, such as hexahydro-3-(2-methylpropyl)-1,4-diaza-2,5-dioxo-3-isobutyl bicyclo [4.3.0] nonane and pyrazine-1,4-dione, using GC-MS analysis, has demonstrated a synergistic effect on biofilm formation. These molecules have antibacterial and antibiofilm properties, which reduce the number of sessile cells. Electrochemical measurements showed that adding the SE reduced the MIC rate, as indicated by an increase in $R_{po}$ and $R_{ct}$ after 7 days of incubation. This study was validated by an in-silico analysis, which showed that the primary molecules in the extract had a strong affinity with the proteins of *P. aeruginosa.* This affinity suggests that the active molecules directly interact with the bacterial proteins, reducing the coupon's corrosion and contributing to the observed antibiofilm and antibacterial effects.

## References

[1] K.A. Natarajan, in Biotechnology of Metals. Elsevier, (2018), 355–393. https://doi.org/10.1016/B978-0-12-804022-5.00012-8

[2] H.A. Videla, Microbially induced corrosion: an updated overview. International biodeterioration & biodegradation, 48(1-4), (2001) 176-201. https://doi.org/10.1016/S0964-8305(01)00081-6

[3] M.F. Libert, O. Bildstein, La biocorrosion: Nouvelles approches. Actual Chim. 400–401, (2015) 105. https://new.societechimiquedefrance.fr/wp-content/uploads/2019/12/2015-400-401-oct.-nov.-p105-libert-hd.pdf

[4] NACE International, (2025).The National Association of Corrosion Engineers (NACE). https://inspectioneering.com/tag/nace http://impact.nace.org/

[5] A. Abdolahi, E. Hamzah, Z. Ibrahim, S. Hashim, Microbially influenced corrosion of steels by Pseudomonas aeruginosa. Corrosion Reviews, 32(3-4), (2014) 129-141. https://doi.org/10.1515/corrrev-2013-0047

[6] D. Cai, J. Wu, K. Chai, Microbiologically Influenced Corrosion Behavior of Carbon Steel in the Presence of Marine Bacteria Pseudomonas sp. and Vibrio sp. ACS Omega 6(5), (2021) 3780-3790. https://doi.org/10.1021/acsomega.0c05402

[7] Z. Liu, T. Cui, Y. Chen, Z. Dong, Effect of Cu addition to AISI 8630 steel on the resistance to microbial corrosion, Bioelectrochemistry, 152,

(2023) 108412. https://doi.org/10.1016/j.bioelechem.2023.108412

[8] J. Morales, P. Esparza, S. González, R. Salvarezza, M.P. Arévalo, Corrosion Science. 34(9), (1993) 1531- 1540. https://doi.org/10.1016/0010-938X(93)90246-D

[9] R. Zhu, G. Xie, Z.A. Qin, X. Tang, J. Cai, J. Yang, Effects of dissolved oxygen accelerated P. aeruginosa on the corrosion mechanism of X70 steel in simulated marine environments. Materials Chemistry and Physics, 334, (2025) 130478 https://doi.org/10.1016/j.matchemphys.2025.130478

[10] M.S. Khan, T. Liang, Y. Liu, Y. Shi, H. Zhang, H. Li, S. Guo, H. Pan, K. Yang, Y. Zhao, Microbiologically Influenced Corrosion Mechanism of Ferrous Alloys in Marine Environment. Metals, 12(9), (2022) 1458. https://doi.org/10.3390/met12091458

[11] D. Xu, J. Xia, E. Zhou, D. Zhang, H. Li, C. Yang, Q. Li, H. Lin, X. Li, K. Yang, Accelerated corrosion of 2205 duplex stainless steel caused by marine aerobic Pseudomonas aeruginosa biofilm. Bioelectrochemistry, 113, (2017) 1-8. https://doi.org/10.1016/j.bioelechem.2016.08.001

[12] Y. Wang, R. Zhang, J. Duan, F. Guan, W. Sand, B. Hou, Extracellular Polymeric Substances and Biocorrosion/Biofouling: Recent Advances and Future Perspectives. International journal of molecular sciences, 23(10), (2022) 5566. https://doi.org/10.3390/ijms23105566

[13] I.B. Beech and J. Sunner, Biocorrosion: towards understanding interactions between biofilms and metals. Current Opinion in Biotechnology, 15(3), (2004) 181-186. https://doi.org/10.1016/j.copbio.2004.05.001

[14] X.L. Li, J. Narenkumar, A. Rajasekar, Y.P. Ting, Biocorrosion of mild steel and copper used in cooling tower water and its control. 3 Biotech 8, (2018)178. https://doi.org/10.1007/s13205-018-1196-0

[15] R. Jia, D. Yang, J. Xu, D. Xu, T. Gu, Microbiologically influenced corrosion of C1018 carbon steel by nitrate reducing Pseudomonas aeruginosa biofilm under organic carbon starvation. Corrosion Science, 127, (2017) 1-9. https://doi.org/10.1016/j.corsci.2017.08.007

[16] Y. Huang, E. Zhou, C. Jiang, R. Jia, S. Liu, D. Xu, T. Gu and F. Wang, Endogenous phenazine-1-carboxamide encoding gene PhzH regulated the extracellular electron transfer in biocorrosion of stainless steel by marine Pseudomonas aeruginosa. Electrochemistry Communications, 94, 9-13. https://doi.org/10.1016/j.elecom.2018.07.019

[17] B. Chugh, Sheetal, M. Singh, S. Thakur, B. Pani, A.K. Singh and V.S. Saji Extracellular electron transfer by Pseudomonas aeruginosa in biocorrosion: a review. ACS biomaterials science & engineering, 8(3), (2022) 1049–1059. https://doi.org/10.1021/acsbiomaterials.1c01645

[18] Y. Li, D. Xu, C. Chen, X. Li, R. Jia, D. Zhang, W. Sand, F. Wang, T. Gu, Anaerobic microbiologically influenced corrosion mechanisms interpreted using bioenergetics and bioelectrochemistry: A review, Journal of Materials Science & Technology, 34(10), (2018) 1713-1718. https://doi.org/10.1016/j.jmst.2018.02.023

[19] Z. Xiao, W. Wang, W. Cui, G. Qin, Marine microbial corrosion inhibition of an in situ formed oxide coating on Ti56Zr44 alloy. Materials Chemistry and Physics, 304, (2023) 127924. https://doi.org/10.1016/j.matchemphys.2023.127924

[20] A. Labena, M.A. Hegazy, R.M. Sami, W.N. Hozzein, Multiple Applications of a Novel Cationic Gemini Surfactant: Anti-Microbial, Anti-Biofilm, Biocide, Salinity Corrosion Inhibitor, and Biofilm Dispersion (Part II). Molecules, 25(6), (2020) 1348. https://doi.org/10.3390/molecules25061348

[21] A.A. Jimoh, E. Booysen, L. van Zyl, M. Trindade, Do biosurfactants as anti-biofilm agents have a future in industrial water systems?. Frontiers in Bioengineering and Biotechnology, 11, (2023) 1244595. https://doi.org/10.3389/fbioe.2023.1244595

[22] R.A. Shamsuddin, M.H. Abu Bakar, W.R. Wan Daud, K.B. Hong, J. Mat Jahim, Can electrochemically active biofilm protect stainless steel used as electrodes in bioelectrochemical systems in a similar way as galvanic corrosion protection?. International Journal of Hydrogen Energy, 44(58), (2019) 30512-30523. https://doi.org/10.1016/j.ijhydene.2019.03.089

[23] H. Jafari, E. Ameri, M.H. Vakili, A. Berisha, Novel Silicon-based schiff-base as corrosion inhibitor for anti-corrosion behavior of API 5L Grade B in 1M HCl. Materials Chemistry and Physics, 311, (2024) 128499. https://doi.org/10.1016/j.matchemphys.2023.128499

[24] N. Wang, R. Zhang, K. Liu, Y. Zhang, X. Shi, W. Sand, B. Hou, Application of nanomaterials in antifouling: A review, Nano Materials Science, 6(6), (2024) 672-700. https://doi.org/10.1016/j.nanoms.2024.01.009

[25] R. Mansour, A.M. Elshafei, Role of microorganisms in corrosion induction and prevention. British Biotechnology Journal, 14(3), (2016) 1-11. https://doi.org/10.9734/BBJ/2016/27049

[26] M. Ventura, C. Canchaya, A. Tauch, G. Chandra,

G.F. Fitzgerald, K.F. Chater, D. van Sinderen, Genomics of Actinobacteria: tracing the evolutionary history of an ancient phylum. Microbiology and molecular biology reviews, 71(3), (2007) 495-548. https://doi.org/10.1128/MMBR.00005-07

[27] S. Sengupta, A. Pramanik, A. Ghosh, M. Bhattacharyya, Antimicrobial activities of actinomycetes isolated from unexplored regions of Sundarbans mangrove ecosystem. BMC microbiology, 15(1), (2015)170. https://doi.org/10.1186/s12866-015-0495-4

[28] E.H. Driche, B. Badji, C. Bijani, S. Belghit, F. Pont, F. Mathieu, A. Zitouni, A new saharan strain of Streptomyces sp. GSB-11 produces maculosin and N-acetyltyramine active against multidrug-resistant pathogenic bacteria. Current microbiology, 79(10), (2022) 298. https://doi.org/10.1007/s00284-022-02994-3

[29] N. Goel, M. Ghosh, D. Jain, R. Sinha, S.K. Khare, Inhibition and eradication of Pseudomonas aeruginosa biofilms by secondary metabolites of Nocardiopsis lucentensis EMB25. RSC Medicinal Chemistry, 14(4), (2023) 745-756. https://doi.org/10.1039/D2MD00439A

[30] E.H. Driche, B. Badji, C. Bijani, S. Belghit, F. Pont, F. Mathieu, A. Zitouni, Antibacterial and antibiofilm properties of two cyclic dipeptides produced by a new desert Streptomyces sp. HG-17 strain against multidrug-resistant pathogenic bacteria. International Microbiology, 28(2), (2025) 241–255. https://doi.org/10.1007/s10123-024-00533-7

[31] J.P. Da Rosa, S.R.G. Tibúrcio, J.M. Marques, L. Seldin, R.R.R. Coelho, Streptomyces lunalinharesii 235 prevents the formation of a sulfate-reducing bacterial biofilm. Brazilian Journal of Microbiology, 47(3), (2016) 603–609. https://doi.org/10.1016/j.bjm.2016.04.013

[32] H.A. Videla, L.K. Herrera, Microbiologically influenced corrosion: looking to the future. International microbiology, 8(3), (2005) 169.

[33] K. Alam, A. Mazumder, S. Sikdar, Y.M. Zhao, J. Hao, C. Song, Y. Wang, R. Sarkar, S. Islam, Y. Zhang, A. Li, Streptomyces: The biofactory of secondary metabolites. Frontiers in microbiology, 13, (2022) 968053. https://doi.org/10.3389/fmicb.2022.968053

[34] M.S. Al-Otaibi, A.M. Al-Mayouf, M. Khan, A.A. Mousa, S.A. Al-Mazroa, H.Z. Alkhathlan, Corrosion inhibitory action of some plant extracts on the corrosion of mild steel in acidic media. Arabian Journal of Chemistry, 7(3), (2012) 340–346. https://doi.org/10.1016/j.arabjc.2012.01.015

[35] D. Sivakumar, R. Ramasamy, Y. Thiagarajan, B. Thirumalairaj, U. Krishnamoorthy, M. Haque Siddiqui, N. Lakshmaiya, A. Kumar, M. Shah, Biosurfactants in biocorrosion and corrosion mitigation of metals: An overview. Open Chemistry, 22(1), (2024) 20240036. https://doi.org/10.1515/chem-2024-0036

[36] M. Hayakawa, H. Nonomura, Humic acid-vitamin agar, a new medium for the selective isolation of soil actinomycetes. Journal of Fermentation Technology, 65(5), (1987) 501-509.

[37] E.H. Driche, N. Sabaou, C. Bijani, A. Zitouni, F. Pont, F. Mathieu, B. Badji, Streptomyces sp. AT37 isolated from a Saharan soil produces a furanone derivative active against multidrug-resistant Staphylococcus aureus. World Journal of Microbiology and Biotechnology, 33, (2017) 105. https://doi.org/10.1007/s11274-017-2265-y

[38] QIAGEN, (2017) DNeasy PowerSoil Kit Handbook. https://www.qiagen.com/us/resources/resourcedetail?id=9bb59b74-e493-4aeb-b6c1-f660852e8d97&lang=en

[39] Bioline, (2023) BIOTAQ DNA Polymerase: Product Information. https://www.bioline.com/biotaq-dna-polymerase.html

[40] S.F. Altschul, W. Gish, W. Miller, E.W. Myers, D.J. Lipman, Basic local alignment search tool. Journal of molecular biology, 215(3), (1990) 403-410. https://doi.org/10.1016/S0022-2836(05)80360-2

[41] O. Trott, A.J. Olson, AutoDock Vina: improving the speed and accuracy of docking with a new scoring function, efficient optimization, and multithreading. Journal of computational chemistry, 31(2), (2010) 455-461. https://doi.org/10.1002/jcc.21334

[42] C. Van Anh, J.S. Kang, J.W. Yang, J.H. Kwon, C.S. Heo, H.S. Lee, C.H. Park, H.J. Shin, Sesquiterpenes from Streptomyces qinglanensis and their cytotoxic activity. Marine Drugs, 21(6), (2023) 361. https://doi.org/10.3390/md21060361

[43] N. Anita, R.M. Joany, R. Dorothy, J. Aslam, S. Rajendran, A. Subramania, G. Singh, C. Verma, Chapter 4 - Linear polarization resistance (LPR) technique for corrosion measurements. Electrochemical and Analytical Techniques for Sustainable Corrosion Monitoring, Advances, Challenges and Opportunities, Elsevier, (2023) 59-80. https://doi.org/10.1016/B978-0-443-15783-7.00005-0

[44] L. Cockenpot, (2014) Mechanisms of Antibiotic Resistance of Pseudomonas aeruginosa in Swarming Motility and its Ecological Function, Master's thesis, Institut Armand-Frappier, INRS, Canada. https://espace.inrs.ca/id/eprint/3306/1/Laure%20Cockenpot.pdf

[45] W. Wenkai, S. Zhihua, W. Jiajia, D. Zhang, P. Wang, C. Li, L. Zhu, Y. Gao, Y. Sun, The Nitrate-Dependent Impact of Carbon Source Starvation on EH40 Steel Corrosion Induced by the

Coexistence of Desulfovibrio vulgaris and Pseudomonas aeruginosa. Metals, 13(12), (2023) 413. https://doi.org/10.3390/met13020413

[46] S. Wu, Q. Jiang, C. Liu, R. Xie, J. Duan, B. Hou, Inhibition of carbon steel corrosion caused by Pseudomonas aeruginosa biofilms using the eco-friendly ε-Polylysine antimicrobial peptide. Corrosion Science, 236, (2024) 112228. https://doi.org/10.1016/j.corsci.2024.112228

[47] A. Timoncini, L. Lorenzetti, R.J. Turner, A. McGibbon, C. Martini, E. Cofini, E. Bernardi, C. Chiavari, Inhibition of Pseudomonas aeruginosa biofilm formation on copper-based thin foils. Plos One, 19(12), (2024) e0314684. https://doi.org/10.1371/journal.pone.0314684

[48] E. Asimakopoulou, S.I. Ekonomou, P. Papakonstantinou, O. Doran, A.C. Stratakos, (2021). Inhibition of corrosion causing Pseudomonas aeruginosa using plasma-activated water. Journal of Applied Microbiology, 132(4), (2021) 2781-2794. https://doi.org/10.1111/jam.15391

[49] R.M. Bethea, (2018). Statistical methods for engineers and scientists. CRC Press. https://doi.org/10.1201/9780203738580

[50] M.B. Ives, J.L. Luo, J.R. Rodda, (2001). Passivity of metals and semiconductors: Proceedings of the Eighth International Symposium. The Electrochemical Society.

[51] Thermo Scientific Chemicals. (n.d.). 1,3-dioxane, 98% [Product datasheet]. Fisher Scientific. https://www.fishersci.fr/shop/products/1-3-dioxane-98-thermo-scientific/15410498

[52] J. Badoz Lambling, J.C. Bardin, Solvation of ions by nitromethane. Electrochimica Acta, 19(11), (1974) 725–731. https://doi.org/10.1016/0013-4686(74)80015-0

[53] National Institute of Standards and Technology. (n.d.). Hydrazine, 1, 2 dimethyl. NIST Chemistry WebBook, SRD 69. https://webbook.nist.gov/cgi/cbook.cgi?ID=540738

[54] M.H. Mohamad, R. Awang, W.M. Yunus, A review of acetol: Application and production. American Journal of Applied Sciences, 8(11), (2011) 1135–1139. https://doi.org/10.3844/ajassp.2011.1135.1139

[55] N. Liang, V. Neužil-Bunešová, V. Tejnecký, M. Gänzle, C. Schwab, 3-Hydroxypropionic acid contributes to the antibacterial activity of glycerol metabolism by the food microbe Limosilactobacillus reuteri. Food Microbiology, 98, (2021) 103720. https://doi.org/10.1016/j.fm.2020.103720

[56] J.P. Kamerling, 1.01 - Basics Concepts and Nomenclature Recommendations in Carbohydrate Chemistry. Comprehensive glycoscience: From chemistry to systems biology, 1, (2007) 1-38. https://doi.org/10.1016/B978-044451967-2/00001-5

[57] P. Seboletswe, P. Awolade, P. Singh, Recent developments on the synthesis and biological activities of fused pyrimidinone derivatives. ChemMedChem, 16(13), (2021) 2050–2067. https://doi.org/10.1002/cmdc.202100083

[58] L.N. Mander, (1991). Naphthoic acids. In Comprehensive Organic Synthesis. Pergamon Press.

[59] R.S. Vardanyan, V.J. Hruby, (2006). Synthesis of essential drugs. Elsevier.

[60] M. Manimaran, K. Krishnan, Marine Sp. VITMK1 derived pyrrolo[1,2-a]pyrazine-1,4-dione, hexahydro-3-(2-methylpropyl) and its free radical scavenging activity. The Open Bioactive Compounds Journal, 5(1), (2017) 23–30.

[61] A.A. Al-Askar, F.O. Alotibi, G.A. Abo-Zaid, A. Abdelkhalek, Pyrrolo[1,2- a]pyrazine1,4-dione, hexahydro-3-(2-methylpropyl), as the primary secondary metabolite of Bacillus spp., could be an effective antifungal agent against the soil-borne fungus, Sclerotium bataticola. Egyptian Journal of Chemistry, 67(13), (2024) 1009–1022.

[62] G.N. Rajivgandhi, G. Ramachandran, C.C. Kanisha, J.L. Li, L. Yin, N. Manoharan, N.S. Alharbi, S. Kadaikunnan, J.M. Khaled, W.J. Li, Anti-biofilm compound of 1,4-diaza-2,5-dioxo-3-isobutyl bicyclo[4.3.0]nonane from marine Nocardiopsis sp. DMS 2 (MH900226) against biofilm forming K. pneumoniae. Journal of King Saud University - Science, 32(8), (2020) 3495–3502. https://doi.org/10.1016/j.jksus.2020.10.012

[63] P.O. Samirana, Y.B. Murti, R.I. Jenie, E.P. Setyowati, GC-MS metabolomic approach to study antimicrobial activity of the marine sponge-derived fungi Trichoderma reesei TV221. Journal of Applied Pharmaceutical Science, 13(7), (2023) 159–173. https://doi.org/10.7324/JAPS.2023.124424

[64] M. Manimaran, J.V. Gopal, K. Kannabiran, Antibacterial activity of Streptomyces sp. VITMK1 isolated from mangrove soil of Pichavaram, Tamil Nadu, India. Proceedings of the National Academy of Sciences, India Section B: Biological Sciences, 87(2), (2017) 499-506. http://dx.doi.org/10.1007/s40011-015-0619-5

[65] G. Rajivgandhi, G. Ramachandran, M. Maruthupandy, B. Vaseeharan, N. Manoharan, Molecular identification and structural characterization of marine endophytic actinomycetes Nocardiopsis sp. GRG 2 (KT 235641) and its antibacterial efficacy against isolated ESBL producing bacteria. Microbial Pathogenesis, 126, (2019) 138-148. https://doi.org/10.1016/j.micpath.2018.10.014

[66] G.M. Morris, R. Huey, W. Lindstrom, M.F. Sanner, R.K. Belew, D.S. Goodsell, A.J. Olson, AutoDock4 and AutoDockTools4: Automated docking with selective receptor flexibility. Journal of computational chemistry, 30(16), (2009) 2785-2791. https://doi.org/10.1002/jcc.21256

[67] C.Q. Hu, K. Li, T.T. Yao, Y.Z. Hu, H.Z. Ying, X.W. Dong, Integrating docking scores and key interaction profiles to improve the accuracy of molecular docking: Towards novel B-RafV600E inhibitors. MedChemComm, 8(9), (2017) 1835–1844. https://doi.org/10.1039/c7md00229g

## Authors Contribution Statement

F. Bouchakour: Conceptualization, Methodology, Investigation, Formal analysis, Data curation, Writing – Original Draft. E. Driche: Methodology, Validation, Formal analysis, Writing – Review & Editing. C. Fares: Methodology, Validation, Formal analysis, Writing – Review & Editing. T. Unsal: Investigation, Software, Interpretation of data, Writing – Review & Editing. O. S. Taskın: Data curation, Interpretation of data. A. Aksu: Data curation, Interpretation of data. M. Sebaihia: Supervision, Validation. All authors have read and agreed to the published version of the manuscript.

## Declaration of generative AI and AI-assisted technologies in the writing process

The authors declare that ChatGPT-5.1 (OpenAI) was used solely for language polishing, grammar correction, and enhancing clarity and readability of the manuscript. All scientific content, experimental data, analyses, interpretations, and conclusions in this study are entirely original and generated by the authors.

## Funding

The authors declare that no funds, grants or any other support were received during the preparation of this manuscript.

## Competing Interests

The authors declare that there are no conflicts of interest regarding the publication of this manuscript.

## Data Availability

The data supporting the findings of this study can be obtained from the corresponding author upon reasonable request.

## Has this article screened for similarity?

Yes

## About the License